CHARM PRODUCTION AND FRAGMENTATION*

J. Chapman

University of Michigan
Ann Arbor, Michigan

*Work supported in part by U.S. Department of Energy contract number DoE Contract DE-AC02-76ER01112.

INTRODUCTION

The observation of charm states at PEP energies is of interest as a means of testing the current ideas of quark production and hadronization in e^+e^- interactions. In addition the observation of new states serves to extend the spectroscopy of bound charm states. The picture that summarizes the production mechanism is the familiar one shown in Figure 1. The interaction proceeds through either the photon or Z° and materializes as a quark-antiquark pair. For the production of charm (anticharm) quarks this primary pair must be the observed charm in the final state or a "b" quark (antiquark) which decays dominantly into charm (anticharm). If the initial quark pair is the charm (anticharm) which appears in the final state, the production is referred to as direct. The charm quarks produced either directly or through decay are observed as bound states with light quarks (D states) or with strange quarks (F states). The cross sections for the various D and F states serve as a measure of the population of light and strange quarks in the sea and of the binding of charm into pseudoscalar and vector states. In what follows the standard convention of writing only the particle state will be adopted. The reader should attach the term "plus charge conjugate" to all states since the data has been treated symmetrically with respect to charge conjugate states. Data is presented from the PEP detectors MKII,[1] TPC,[2] HRS,[3] MAC,[4] and DELCO.[5] Summary plots and tables also contain data from CLEO,[6] ARGUS,[7] TASSO,[8] MARK-J,[9] JADE,[10] CDHS,[11] E531,[12] and several summary reports.[13]

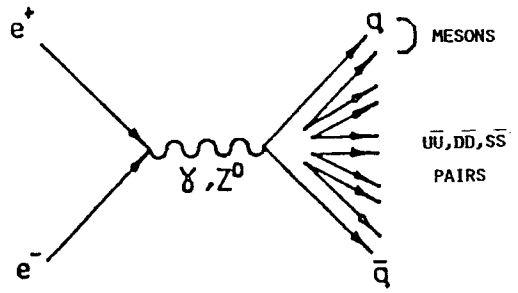

Figure 1. The primary production mechanism of hadronic events in e^+e^- interactions showing the intermediate state as either a photon or Z°.

D STATES

The production of D and D^* mesons has been observed to dominate the final states with charm. These D states are directly produced and are energetic since they carry the heavy quark that left the interaction with 1/2 the collision energy.

The detection of D^* final states is aided by the very low Q of the D^* decay to D. A plot of the mass difference between the two states results in the appearance of the dramatic peak shown in Figure 2 for data from the TPC collaboration. Here the final states for the D^{*+} decay to $D^\circ\pi^+$ is plotted for several decay modes of the D°. The data from the TPC are included along with similar data from other detectors in the summary plots of D^* cross sections and fragmentation distributions of Figures 4 and 5.

The D° and D^+ signals are not as readily extracted. Without the small mass difference to aid in the suppression of background, one must rely, as does the HRS group, on exceptional mass resolution. The HRS data for the D° and D^+ is shown in Figures 3a and 3b. The data of plots 3a and 3b has been restricted to a limited range of D decay angle as a means of further reducing the background. These data also appear in the summary plots of Figures 4 and 5.

The D and D^* data corrected for acceptance and branching fraction[14] is summarized in Figure 4. The cross section is plotted in terms of its ratio to the $\mu\mu$ cross section. The plot also contains the lines that represent the expected contribution from direct charm and charm from b decays. It is clear that the production of D and D^* states can account for essentially all of the

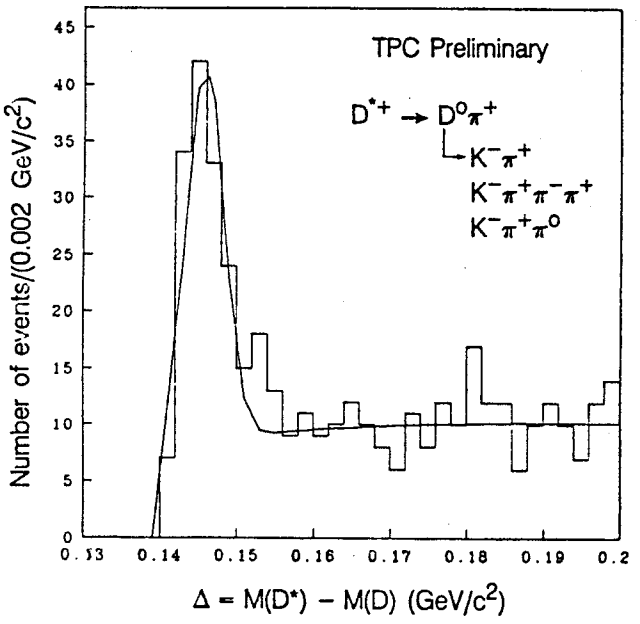

Figure 2. The mass difference plot from the TPC collaboration for D^* event selection. Several decay modes of the D° are included as indicated on the plot.

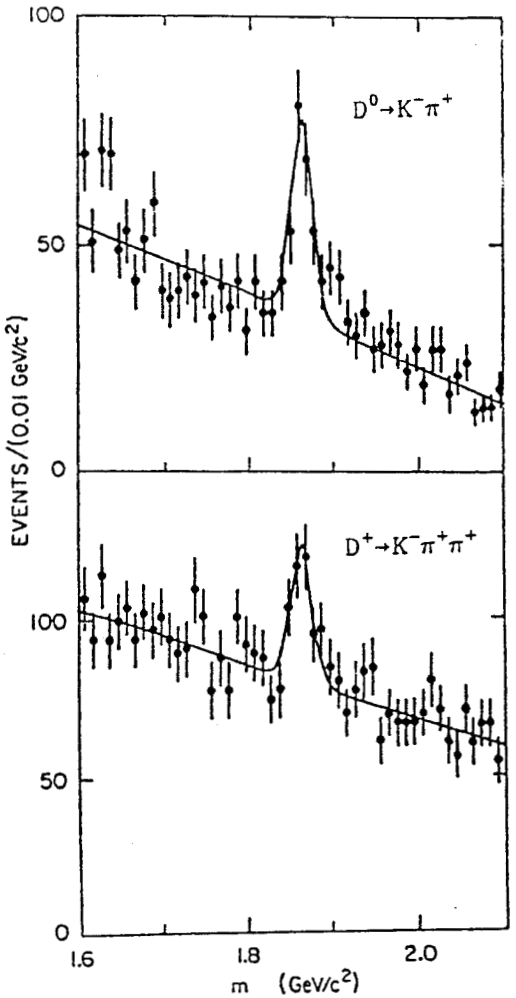

Figure 3. The mass plots D° and D^+ from the HRS collaboration. The exceptional resolution of the HRS permits a study of the D independent of any intermediate D*. The data is restricted to $z_D > 0.5$ and $|\cos \theta^*| < 0.7$.

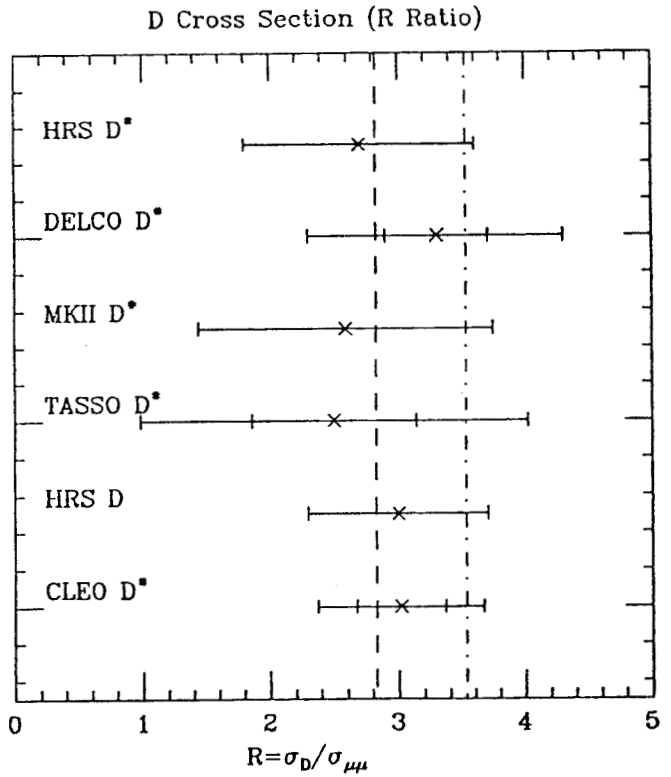

Figure 4. The Cross Section for D and D^* mesons relative to the μμ cross section from various experiments. The dashed line is at 2.83, the value for directly produced charm and the dot-dashed line at 3.53, the value expected for total charm including b decays to charm.

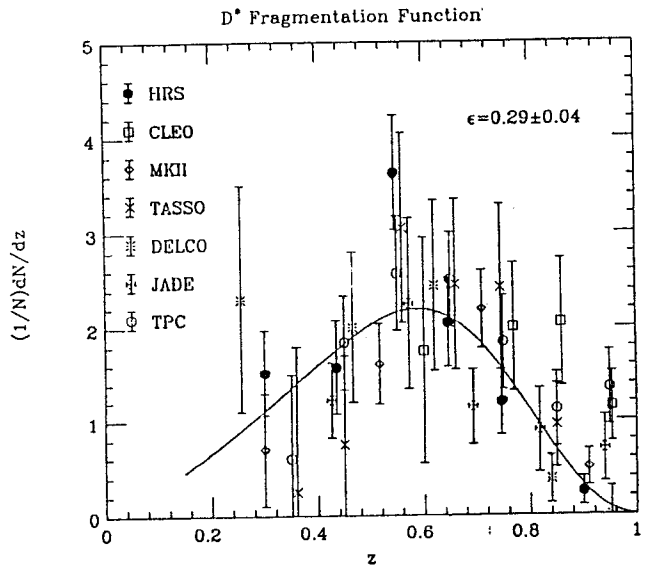

Figure 5. The distribution of D^* events in the fragmentation variable z. The curve is a fitted Peterson form with an ϵ parameter equal to 0.29 ± 0.04.

charm production. The errors from the various experiments are correlated since the largest contribution is due to uncertainties in the decay rates. The independent measurement of D and D^* cross sections by the HRS permits a determination of the D/D^* ratio. The value of D/D^* for $z > 0.5$ is 1.0 + 0.3 - 0.2. This range is consistent with the earlier published number from the CLEO collaboration of 1.18 ± 0.4 and is consistent with both D^* domination (1.0) and the ratio predicted by spin state counting (1.33).

A frequently used variable that characterizes the production energy spectrum is the fractional energy, z, of the particle relative to 1/2 the collision energy. Peterson et al.[15], have represented the distribution function, D(z), for heavy quark particles as,

$$D(z) \sim A/z^2[1 - 1/z - \epsilon/(1 - z)]^{-2}.$$

The parameter, ϵ, should be a falling function of the heavy quark mass. The D* data have been used to determine the fragmentation function, D(z), for charm as shown in Figure 5. Again data from numerous experiments have been included. The curve shown is a fit to the Peterson form. The fit yields a value for the "ϵ" parameter of 0.29 ± .04. The fit quality is good indicating that the data is well represented by the form. A mean value for the fragmentation variable, z, is also derived from the data. A graph of these mean values is shown as Figure 6. The weighted average of the individual mean values is 0.58 ± .02.

The interference between charm production through the photon with charm produced through the Z° results in a forward-backward

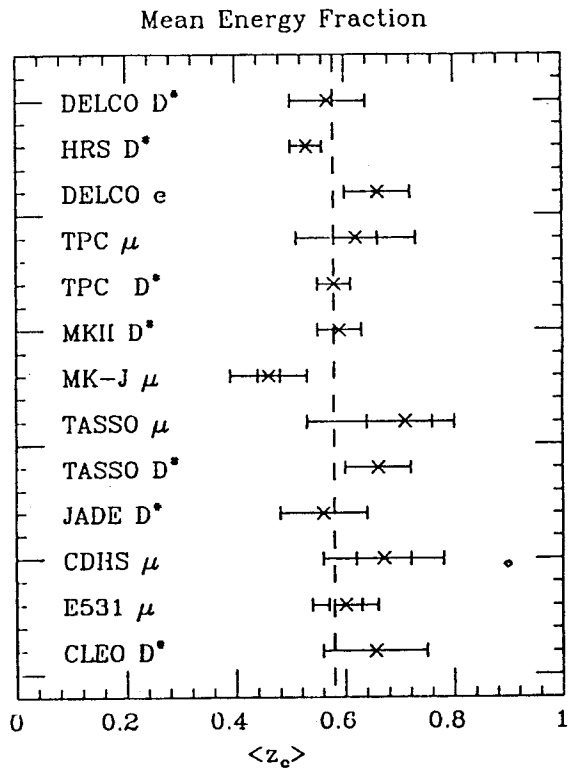

asymmetry that is predictable in the standard model. Measurements of the asymmetry serve as a test of the prediction. The asymmetry for charm quarks represented as

$$A = (N_+ - N_-)/(N_+ + N_-)$$

is predicted by the model to be

A = -9% at PEP (29 GeV) and A = -14% at PETRA (34 GeV).

The number N^+ represents the count of events with the outgoing quark in the hemisphere of the incoming e^- particle and N_- represents the count of antiquark in that hemisphere. For D and D^* production, the D state is a sufficient measure of the initial quark direction since the D's are very fast (mean z ~ 0.6). The D and D^* data has been tested for consistency with the standard model. The asymmetry measurements from PEP and PETRA detectors are summarized in Figure 7. The expected values are also shown as the dashed lines. Agreement is obviously very good at the current measurement accuracy.

The presence of D events is also observed through the semileptonic decay of the D to both electrons and muons. Events of this type are observed to produce leptons at large p_t to the D jet axis. Yet larger p_t leptons are produced by B events and are statistically separable from the D generated leptons. Several PEP and PETRA detectors have measured the semileptonic branching fraction, mean value of the fragmentation variable, and electroweak asymmetry from such leptonic final states. Figure 7 contains the asymmetry measurements and Figure 8 the semileptonic branching fractions.

The presence of separable D* final states serves as an event tag for e^+e^- interactions where charm is directly produced. With

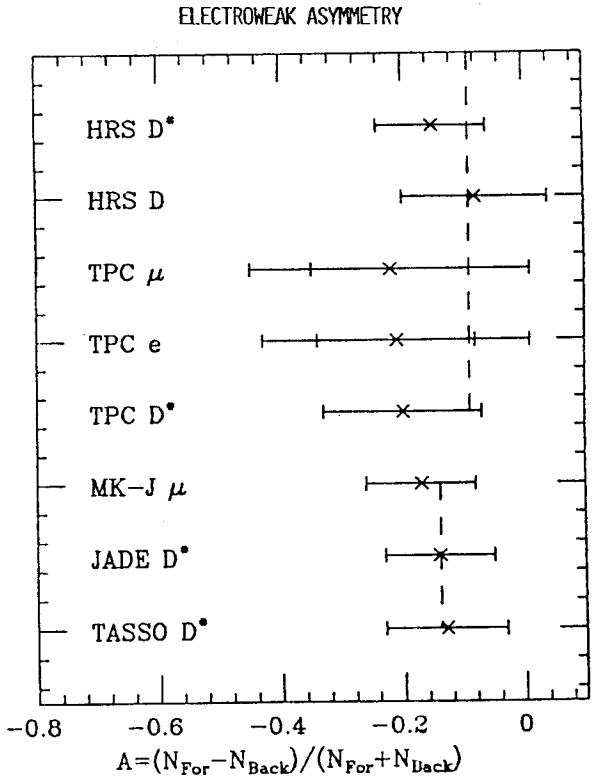

Figure 7. The electroweak asymmetry for charm as measured with the charm tags of D mesons.

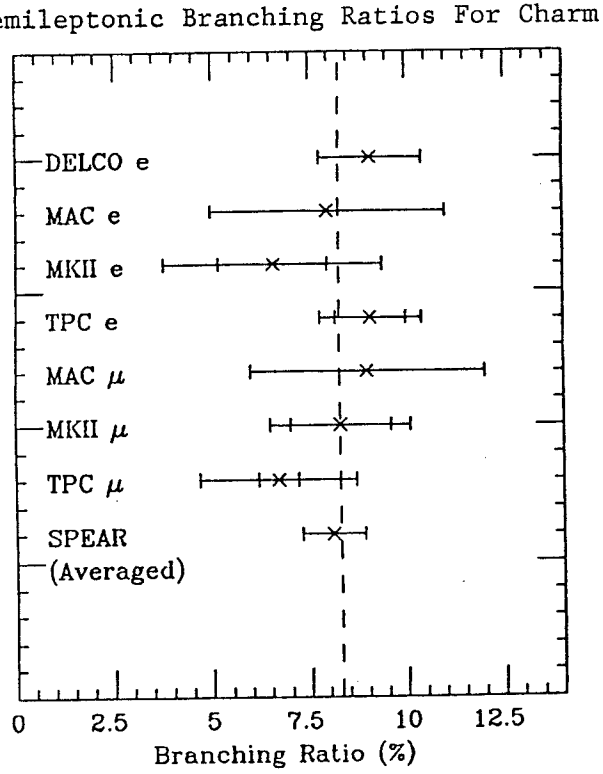

Figure 8. The semileptonic branching fractions for charm. The dashed line is the 8.3 ± 0.5 average of several PEP and PETRA detectors and the SPEAR average shown.

this charm tag and an equivalent tag of light quark events, one is able to do comparisons of the hadronization characteristics of two distinct initial quark samples. The HRS group has accomplished such a separation using a D^* tag for charm and a single fast track tag for light quark events. The multiparticle decay kinematics of heavy quark mesons suppresses the generation of decay products with z values approaching 1.0 relative to the number of light quark fragments at high z. A comparison of kinematic variable averages for the two samples is given in Table 1. Plots 9a and 9b illustrate the distributions in two of the variables for the samples. In the case of the average p_t^2 the samples show no differences. The average multiplicity differs in the two samples but the distributions when scaled by the averages are the same within errors. The results are in qualitative agreement with the results of a comparison of D^* events with all events done by the TASSO collaboration.

F STATES

An F state 1975 MeV/c^2 has been observed in several other detectors since its first observation by the CLEO collaboration about a year ago. The original observation in the $\phi\pi$ final state is shown in Figure 10. This observation was restricted to F mesons produced at momenta greater than 2.5 GeV/c^2 in order to remove events produced through B states. The F mesons were found to be consistent with direct charm production. A branching fraction of 4.4% to $\phi\pi$ was calculated under the assumption that the rate of F production was 15% of the total direct charm as is typical of s quark extraction from the sea. Observations by TASSO in the same

TABLE OF VARIABLE AVERAGES

VARIABLE	CHARM	LIGHT QUARK
$\Sigma\|P\|$	8.57±.03	8.98±.02
$\langle N_{CH}\rangle$	6.67±.21	5.84±.13
$\langle P\rangle$	1.41±.05	1.51±.04
$\langle P_T^2\rangle$	.20±.02	.23±.02
$\langle S\rangle$	.097±.01	.100±.007
$\langle 1-T\rangle$	.040±.003	.037±.002

TABLE I

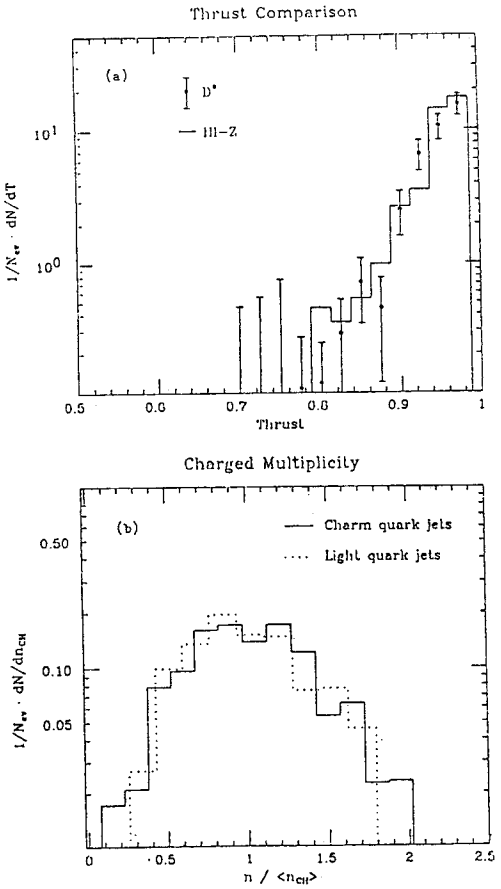

Figure 9. The distributions in (a) thrust and (b) scaled multiplicity for the charmed tagged and light quark tagged event samples.

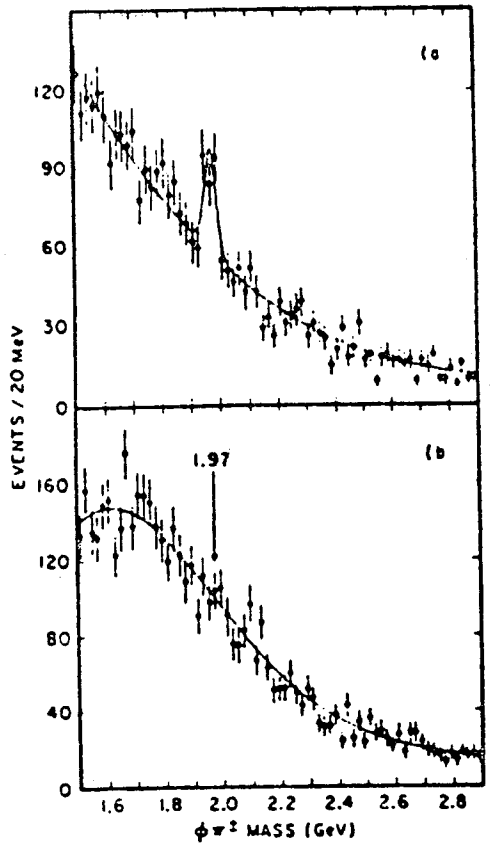

Figure 10. The F 1975 signal as first seen by the CLEO collaboration in the $\phi\pi$ mass spectrum for (a) true $\phi\pi$ candidates and (b) $\phi\pi$ candidates where the "ϕ" is chosen above and below the ϕ mass.

final state (shown later with HRS data) were qualitatively similar but with a rate that implies a 13% branching fraction.

The resolution of the HRS permits the extraction of an F signal over a wider z range than TASSO. The ϕ signal shown in Figure 11 illustrates this exceptional resolution. The ϕ cross section extracted from the data of Figure 11 is plotted in Figure 12 along with data from TPC and DELCO. The agreement between experiments and with the Lund Monte Carlo[16] is good. The ϕ events from the HRS are combined with the remaining tracks of the events to obtain the plot of Figure 13. The prominent peak at $\phi\pi$ mass of 1975 MeV/c^2 is clear. The width of 16 MeV/c^2 is consistent with the resolution of the HRS. The F signal as a function of z is extracted from the data of Figure 13 and is shown in Figure 14. The most striking feature of Figure 14 is the low peaking near z = .25. Such low values of the fragmentation variable are more characteristic of F mesons from B decay than from direct charm production. The amount of F produced at high z is lower than that from the TASSO experiment (also shown on Figure 14) but is consistent with the CLEO results. The HRS would calculate a branching fraction near the CLEO value from the high z data alone. The curve on Figure 14 is an estimate of the direct charm generated F events. The shape is taken from the fragmentation function of the D^* data and the normalization from a scaling of the CLEO result with energy. The large low z peak suggest a B meson source for F events but is surprisingly large considering the factor of four fewer b than c quarks in e^+e^- interactions. The decay angular distributions for the F as extracted by the HRS are shown in Figure

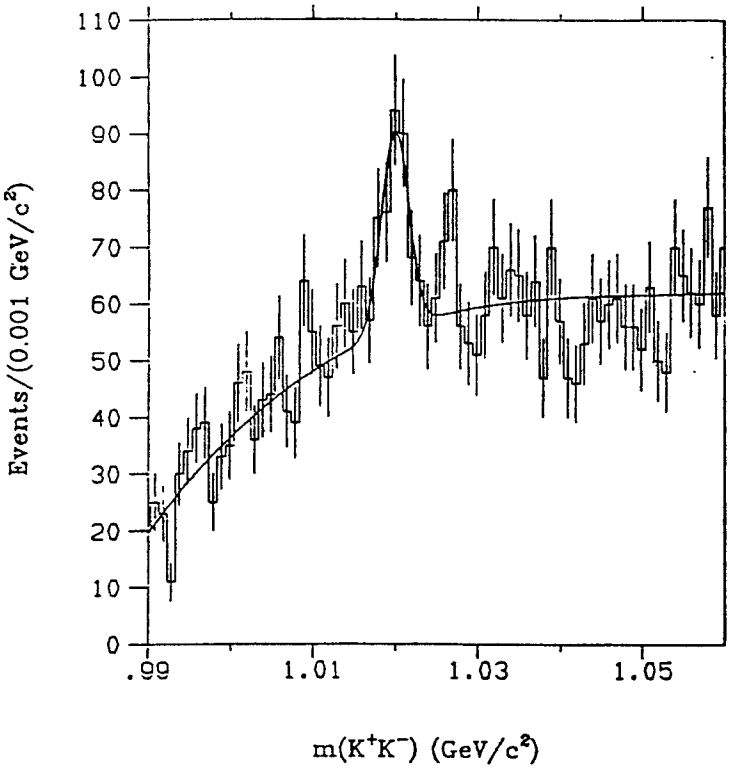

Figure 11. The K^+K^- mass spectrum from the HRS detector showing a 5.8 MeV/c^2 wide peak at the ϕ mass.

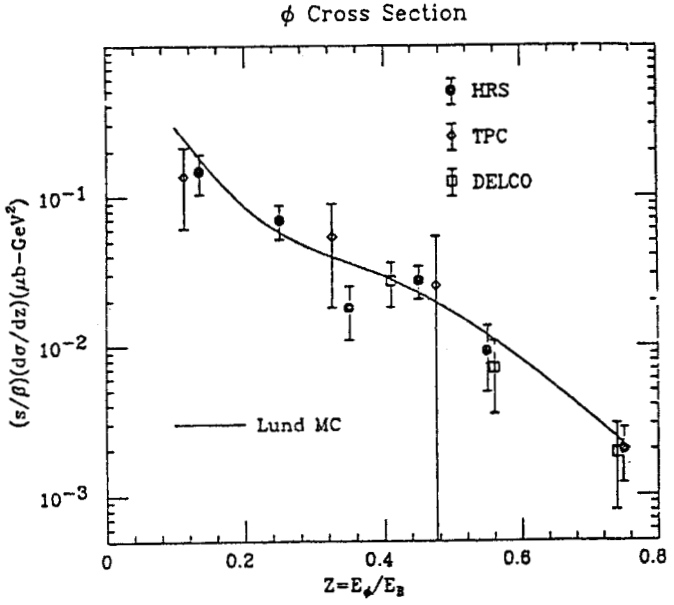

Figure 12. The ϕ differential cross section as measured by the HRS, TPC and DELCO along with the Monte Carlo simulation of the LUND program.

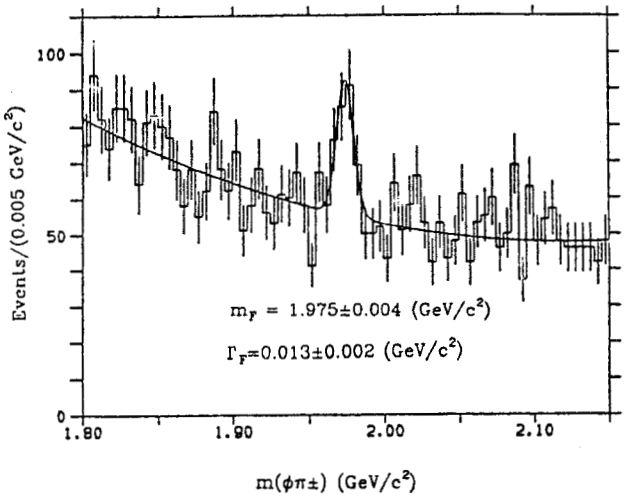

Figure 13. The $\phi\pi$ mass spectrum from the HRS collaboration. The peak at 1975 MeV/c^2 is interpreted as the F seen by CLEO.

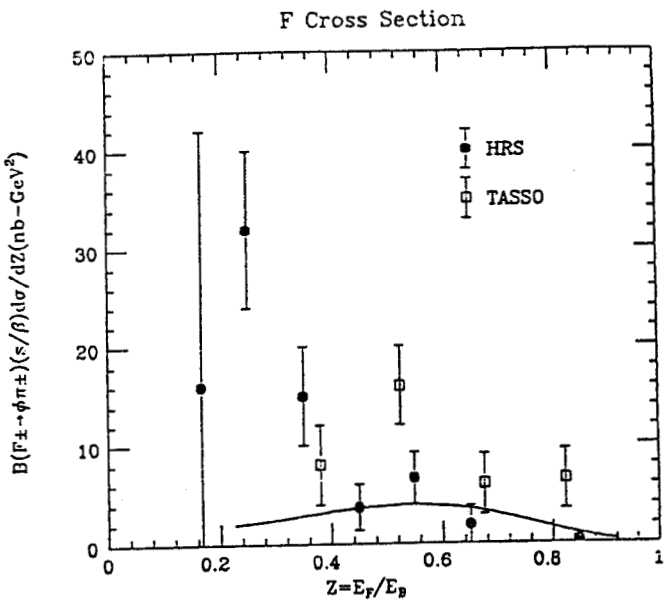

Figure 14. The branching ratio times cross section as a function of the fragmentation variable, z. The data comes from HRS and TASSO. The curve is an estimate of the direct charm signal extrapolated from the CLEO data and distributed according to a D type fragmentation function.

15 along with the expected forms for a pseudoscalar meson decaying to a vector ϕ and a pseudoscalar π. The data are better represented by the background at large z than by the predicted F shape. The data is mostly at low z where the F shape and the background are nearly the same. Conclusive decay angle tests must await additional data.

The TPC collaboration has reported observation of an F^* resonance decaying to an F and a photon. The data is illustrated in Figure 16b. The $KK\pi$ invariant mass is plotted in 16a for three event selections. Figure 16b shows the mass difference of the $KK\pi\gamma$ mass minus the $KK\pi$ mass in a manner reminiscent of the D^* - D mass difference technique. If the mass difference is restricted to the low peak of 16b, an F signal is more clearly visible in 16a. This restricted sample is labeled the F^* region in the plot of Figure 16a. A selection of mass differences in the control region does not show an F signal. The TPC F is seen in $KK\pi$, not $\phi\pi$, in contrast to the observations of the other detectors. The TPC acceptance for $\phi\pi$ is small since particle identification is needed and the low Q of the ϕ decay results in a loss of ionization information.

The ARGUS collaboration has recently presented evidence for an F^* decaying into F and a photon. The F is observed in the $\phi\pi$ final state. Figure 17 shows the ARGUS data plotted as a distribution in $\phi\pi$ invariant mass with and without selection of the $\phi\pi\gamma$ (F^*) mass in the region 2.08 to 2.17 GeV/c^2. The F signal is enhanced by the F^* selection without appreciable reduction in size.

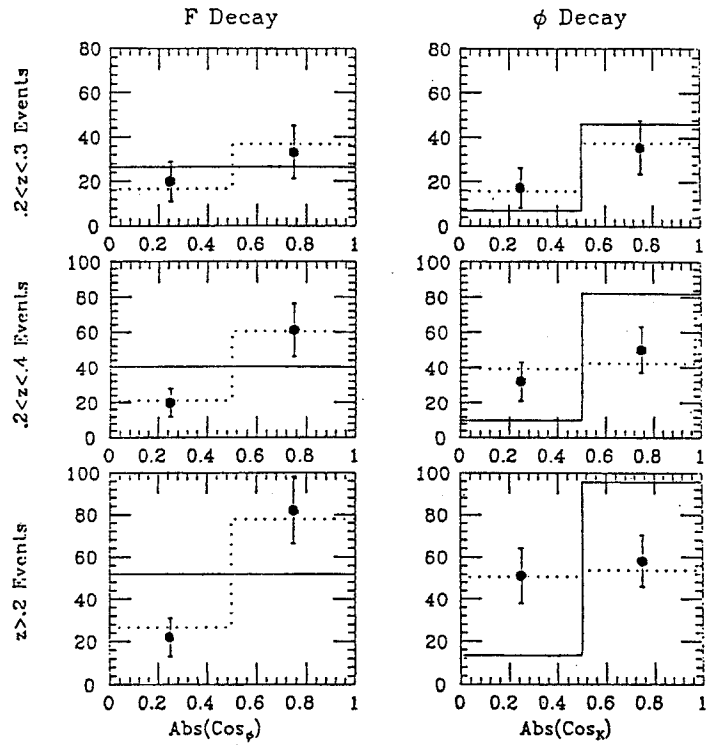

Figure 15. The decay angular distributions for the F and ϕ from the F for three overlapping ranges of the fragmentation variable z. The solid histogram represents the expected distributions for a pseudoscalar decay to a vector and a pseudoscalar. The dashed curve is the measured distribution of the background under the F. The data points appear as dots with error bars.

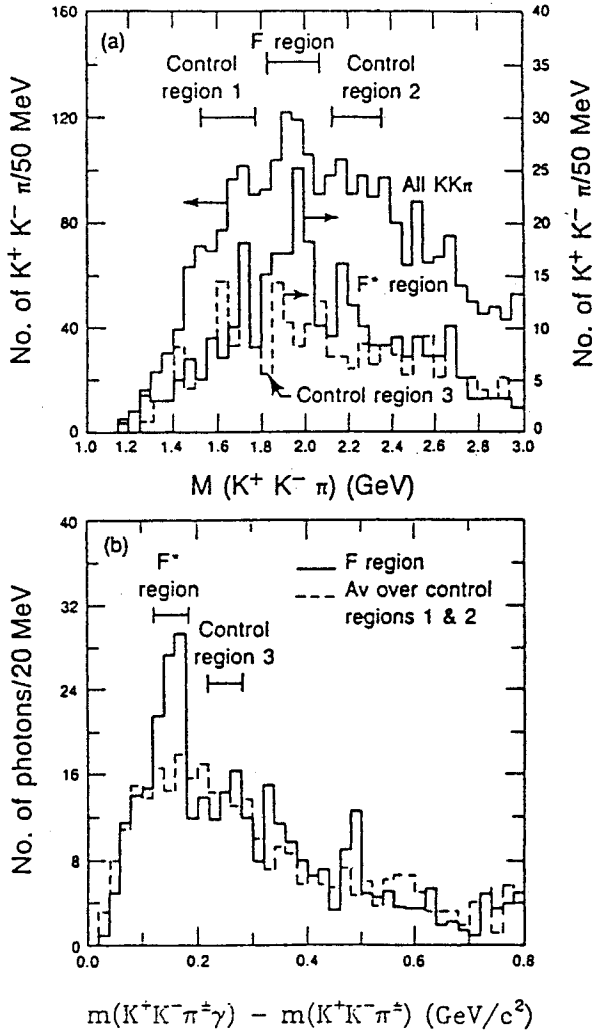

Figure 16. The invariant mass of (a) the $K^+K^-\pi^\pm$ and (b) the $K_+K_-\pi_\mp\gamma$ - $K_+K_-\pi_\mp$ for TPC data. Particle identification has been used to select combinations consistent with the assigned particles.

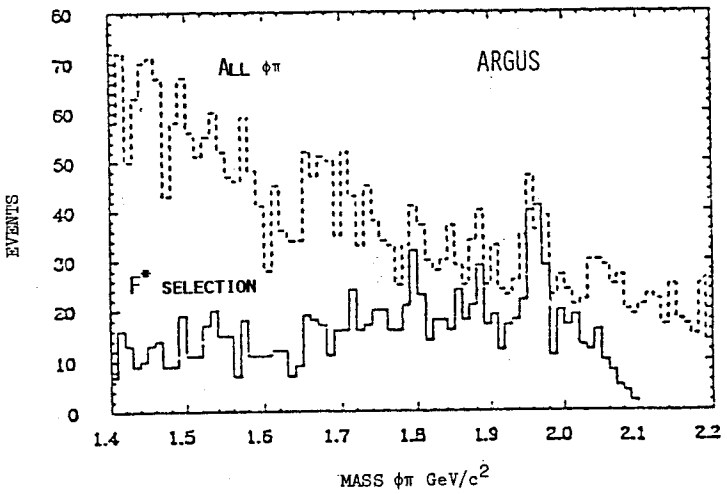

Figure 17. The $\phi\pi$ invariant mass with and without selection of an F^* in the $\phi\pi\gamma$ mass. The dashed histogram is for all $\phi\pi$ and the solid histogram is for 2.08 GeV/c^2 < $M_{\phi\pi\gamma}$ < 2.17 GeV/c^2.

REFERENCES

1. MARKII
M. E. Nelson et al., Phys Rev Lett. 50, 1542 (1983).
M.E. Nelson et al., Preprint LBL-16724 (1983).
Y.M. Yelton et al., Phys Rev Lett. 49, 430 (1982).
Y.M. Yelton, Private Communication (Recent Data).
R. Schindler et al., Phys Rev D24, 78 (1981).

2. TPC
R.J. Madaras, Preprint LBL-17806 (1984).
H. Aihara et al., Preprint LBL-17545 (1984).
H. Aihara et al., Phys Rev Lett. 52, 2201 (1984).
J.A.J. Matthews, Leipzig Conference (1984).
A. Barbaro-Galtieri, Palermo Conference (1984).
W. Hofmann, Vanderbilt Conference (1984).

3. HRS
M. Derrick et al., Preprint HRS-CP-84-2
and Leipzig Conference (1984).
M. Derrick et al., Inclusive D^0 and D^+ Production in e^+e^- Annihilation at 29 GeV, Submitted to Physical Review Letters.
M. Derrick et al., Preprint HRS-CP-84-3
and Leipzig Conference (1984).
P. Kesten, Private Communication (Flavor Tagging).
S. Ahlen et al., Phys Rev Lett. 51, 1147 (1983).

4. MAC
E. Fernandez et al., Phys Rev Lett. 50, 2054 (1983).
H.S. Kaye, SLAC Report SLAC-262 (1983).
M. Piccolo, SLAC Institute, 673 (1983).

5. DELCO
D.E. Koop et al., Phys Rev Lett. 52, 970 (1984).
W. Bacino et al., Phys Rev Lett. 43, 1073 (1979).

6. CLEO
A. Chen et al., Phys Rev Lett. 51, 634 (1983).
P. Avery et al., Phys Rev Lett. 51, 1139 (1983).

7. ARGUS
C.W. Darden, Vanderbilt Conference (1984).
A. Silverman, Leipzig Conference (1984).

8. TASSO
M. Althoff et al., Phys Lett. 136B, 130 (1984).
M. Althoff et al., Phys Lett. 135B, 243 (1984).
M. Althoff et al., Phys Lett. 138B, 317 (1984).
M. Althoff et al., Phys Lett. 126B, 493 (1983).

9. MARK-J
A. Adeva et al., MIT-LBS Report 131 (1983).

A. Adeva et al., Phys Rev Lett. 51, 443 (1983).

10. JADE
W. Bartel et al., Cornell Conference (1983).

11. CDHS
H. Abramowicz et al., Z. Phys. C15, 19 (1982).

12. E531
N. Ushida et al., Phys Lett. 121B, 292 (1983).

13. RECENT REVIEWS
G. Hanson, Brighton Conference, 147 (1983).
W. Hofmann, Vanderbilt Conference (1984).
M. Sakuda, Vanderbilt Conference (1984).
M. Pohl, Palermo Conference (1984).
H. Schneider, Brighton Conference (1983).
J. Lee-Franzini, Palermo Conference (1984).
A. Bohm, Brighton Conference (1983).
B. Naroska, Cornell Conference (1983).

14. $BR(D^\circ \to K^-\pi^+) = 0.03 \pm 0.006$,
$BR(D^+ \to K^-\pi^+\pi^+) = 0.063 \pm 0.011$,
$BR(D^{*+} \to D^\circ\pi^+) = 0.44 \pm 0.10$.

15. C. Peterson et al., Phys Rev. D27, 105 (1983).

16. B Andersson, G. Gustafson, G.Ingelsman and
T. Sjostrand, Comp. Phys. Com 27, 243 (1982).
and 28, 229 (1983).